

Damage Assessment in Pultruded GFRP with AE

D. Crivelli¹, M. Guagliano² and A. Monici³

Abstract: Pultrusion is a process for manufacturing uniform section composite profiles, which allows to obtain structural elements of virtually any length. The use of E-glass fiber allows to obtain a material with a good rigidity-to-weight and strength-to-weight ratio; these features allowed to use these materials in civil structures, such as poles for anti-noise panels and public lighting, also thanks to their insulating properties. However, the knowledge on the damage development of these materials is still uncertain, and this is slowing down their development.

For these reasons, an experimental study on pultruded materials aimed at identifying the damage modes has been developed. A set of glass-fiber reinforced pultruded specimens, with two different configurations of additional random short-fiber layers were investigated in tensile tests. Each specimen was monitored with Acoustic Emission sensors through all the test, until breakage. This allowed to gather data and follow the damage development and evolution in this material. The analysis of the Acoustic Emission data allowed to identify some common stages of the static damage modes, and some differences between the two different configurations. Also, the results will allow to extend the monitoring to full-scale elements, with the purpose of testing and real-time health monitoring of structures.

The results suggest that Acoustic Emission is a suitable technique to monitor the structural health of full-scale elements and for in-situ operations.

Keywords: Pultruded composites, glass fiber, acoustic emission, tensile tests, damage

1 Introduction

Composite materials are being spread in lightweight structures engineering, not only in those fields which traditionally require weight reduction and safety increase, such as aircraft manufacturing, but also in civil engineering where these materials

¹ Politecnico di Milano, Dipartimento di Meccanica, Italy

² Politecnico di Milano, Dipartimento di Meccanica, Italy

³ E. T. S. Sistemi Industriali, Brugherio, Italy

have become interesting because of the weight reduction and the reduction of the costs related to transportation and assembly.

In particular, pultruded glass-fiber reinforced polymers (GFRP) allow the production of structural profiles of virtually any length with a cost-effective production technique [Starr (2000)]. This technique consists of an extrusion of the matrix and the tension of the fiber roving (hence the “pull-” and “-trusion”); this allows an overall good fiber alignment and a finer control on polymerization and fiber-matrix adhesion. To improve the mechanical characteristics of those materials in directions other than the long fiber axis, it is possible to embed in the material an arbitrary number of *mat* layers, which consist of randomly oriented short-fiber layers.

However, these materials’ spreading is being delayed by the limited knowledge on the damage mechanisms of these materials. Some experimental campaigns suggest that a complex damage mechanism involves the fiber and the matrix, with a multi-phase load bearing capacity and stiffness degradation [Jessen and Plumtree (1999)], and that fatigue damage consists in fibers breaking, degradation of matrix and interfacial bond degradation between matrix and fiber [Vergani (2006)].

Anyway, the use of some experimental technique able to monitor the damage development can be suggested with the aim to improve the knowledge about the behavior of this material and also to assess the possibility to monitor the damage evolution on practical applications. Among these latter, Acoustic Emission (AE) is one of the most promising, due to its ability to detect damage evolution in real time while the structure or the specimen is being loaded.

AE is a technique that involves the passive measurement of acoustic waves in the ultrasonic band, which are released by the material during damage development [Finleyson (2003)]. Such signals are related to the damage severity and type; AE also allows to localize the source of such waves by using multiple sensors [Grosse and Ohtsu (2008)], and is particularly promising for the testing of full-scale components [Takeda et al. (2007)], but also for material behavior assessment [Huang et al. (1998)]. Pultruded materials have been tested with the AE technique for insulator rods [Carpenter and Kumosa (2000)], but a more extensive knowledge of damage modes can result from AE analysis of a wider set of samples.

Aim of this research is to better assess the capability of AE to monitor and detect damage development on this material, to develop a full-scale damage monitoring technique which can be used for assessing the health of a structure during its life.

2 Materials and methods

The material tested is a pultruded E-glass fiber reinforced material. The resin and glass fraction are respectively 43% and 57% in weight, including the additional layers of random *mat*.

Two different configurations of such layers were tested, namely MAT2 and MAT3. The MAT2 type consisted of uniaxial glass fibers with a top and bottom random fiber layer; the MAT3 type included an additional layer in the middle of the specimen, named *volumat* (Figure 1).

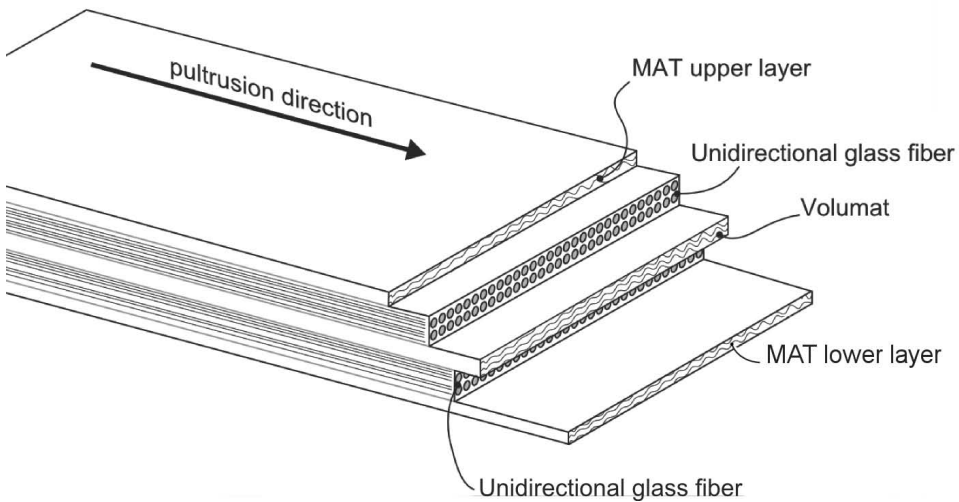


Figure 1: Schematic section of the pultruded MAT3

In Figure 2 the glass-fibers layout can be seen in a 3D tomography image of a MAT2 specimen section, from a previous work of the authors [Crivelli et al. (2010)].

In this work, 15 MAT3 and 19 MAT2 specimens are considered. The specimens were milled to a dog-bone shape (Figure 3). Such configuration allows to avoid the usage of tabs and the consequent stress intensification, and shows the best uniformity in failure mode, position, and avoids unwanted slipping of the tabs due to non-perfect bonding, as experienced by [Keller et al. (2005)]. Each specimen was measured in its smallest section prior to the tensile test.

The specimens were tested in a uniaxial electromechanical testing machine MTS RT100. Tests were made according to [ASTM D3039] in displacement control, with a speed fixed to 2 mm min^{-1} . Displacement was measured through the crosshead position output of the testing machine (being its stiffness much higher

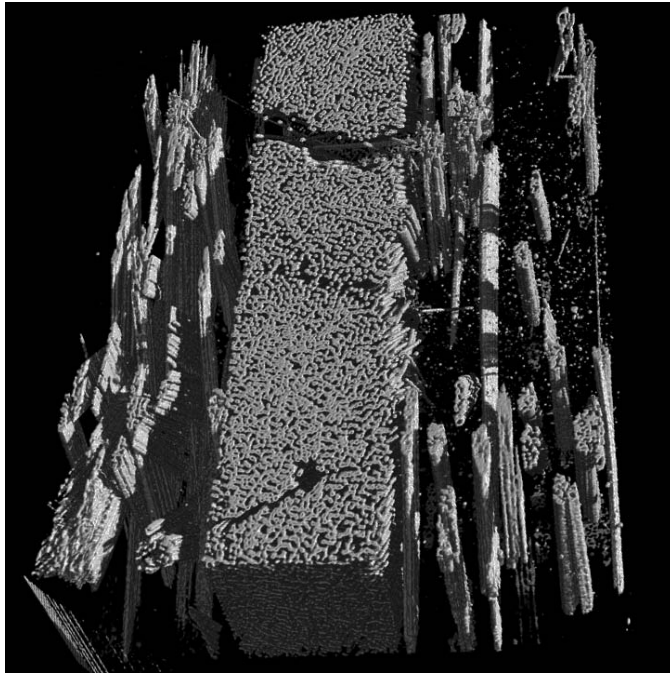


Figure 2: 3D tomography image of a MAT2 specimen cutout (the matrix is filtered)

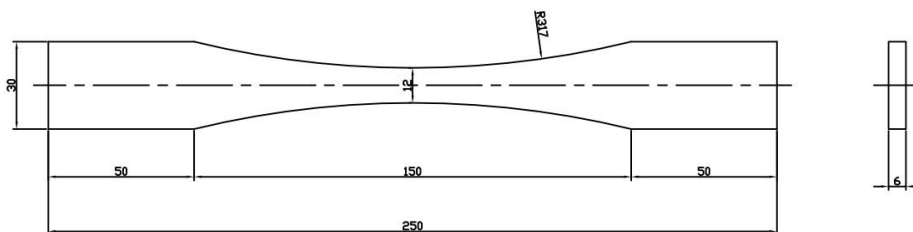


Figure 3: Dogbone specimen geometry (both MAT2 and MAT3)

than the specimen's), and the load was measured with a 100kN load cell.

To monitor the specimens with AE, a commercial instrumentation (Valen AMSY-5) was used. This instrumentation includes the whole measurement chain involved in AE recording (Figure 4).

Two sensors were attached to each specimen with vacuum grease, according to [ASTM E976], at a distance of 120mm. Sensors were then connected to preamplifiers with short cables (less than 1000mm); each preamplifier was connected to one

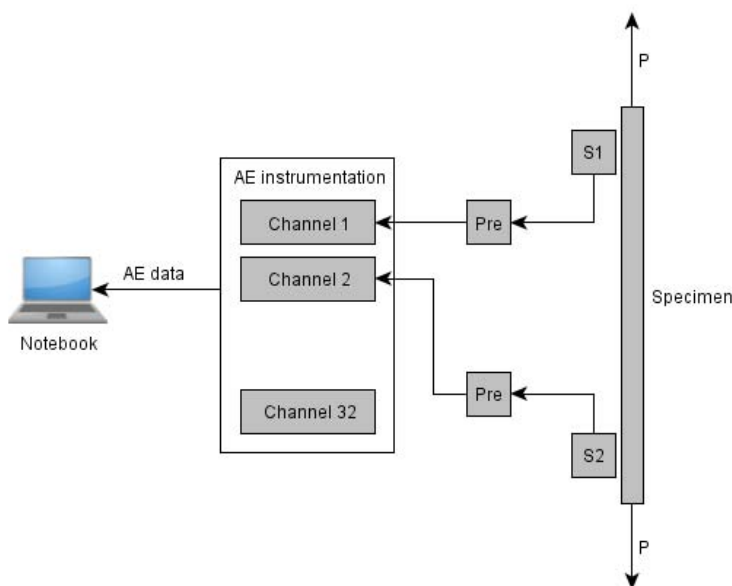


Figure 4: Acoustic Emission data acquisition chain

channel of the AE master unit. The unit was connected to a laptop which recorded the AE “hits” waveforms and parameters (Figure 5). The noise threshold of the channels was set to 40dB AE.

Before each test, the specimen was mounted in the hydraulic grips of the machine. Two minutes of noise were recorded without applying any load, to make sure that no signal would pass the threshold amplitude value.

Then, a “pencil lead break test” [ASTM E976] was performed. This test involves the breakage of a pencil lead at known distances, to assess the signal attenuation as a function of the distance. In this case, the attenuation was less than 5dB over the length of the specimen, and thus it was neglected.

After such tests, the AE system was put in “pulsing” mode. In this phase, each sensor emits a set of signals which are recorded by the other sensor. The time of flight of the signal, calculated as the difference between the emission and the arrival time, is used to calculate the average wave velocity in the material, since the distance between the two sensors is fixed and known. This velocity is then used by the internal algorithms of the AE system to calculate the position of a hit. In

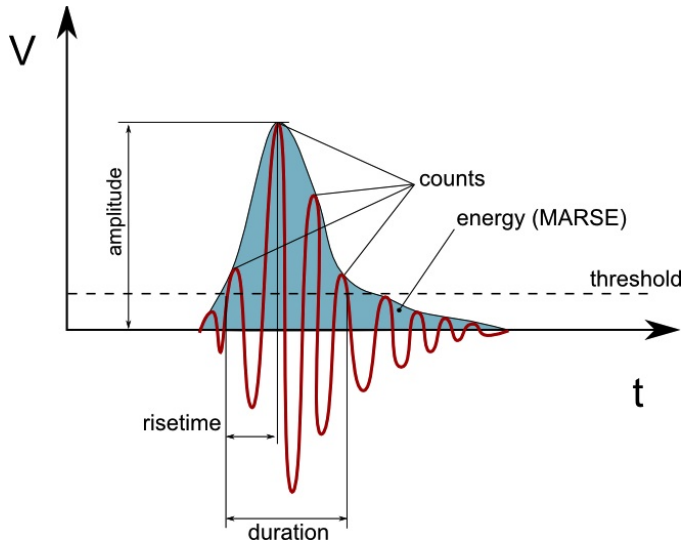


Figure 5: Acoustic Emission signal and parameters example

this case, since the location is performed along a line, the velocity is considered uniform along that line.

After the preparation, the tests were started, and the AE data recorded. The test was stopped when a significant load bearing capacity reduction was seen (namely 20% of the maximum load reached).

After the test was stopped, the AE recording was halted and the specimen was unloaded. The failure mechanism was noted down as suggested by [ASTM D3039]; also the position of the fractures and delaminations was measured and recorded.

3 Results

3.1 Tensile tests

A typical stress-strain curve for a specimen is reported in Figure 6.

It can be seen that the test can be divided into 2 phases: the first, which is almost linear, and a second which presents an inelastic behavior (from a deformation value ε_i) and sudden load bearing drops. This is linked to visible damage development and a sensitive increase in AE activity.

The two materials tested showed a quite uniform behavior, with a tensile strength measured at the first inelastic load drop, with a mean value of about 340 MPa and a standard deviation of 28 MPa (Figure 7). No significant difference between the

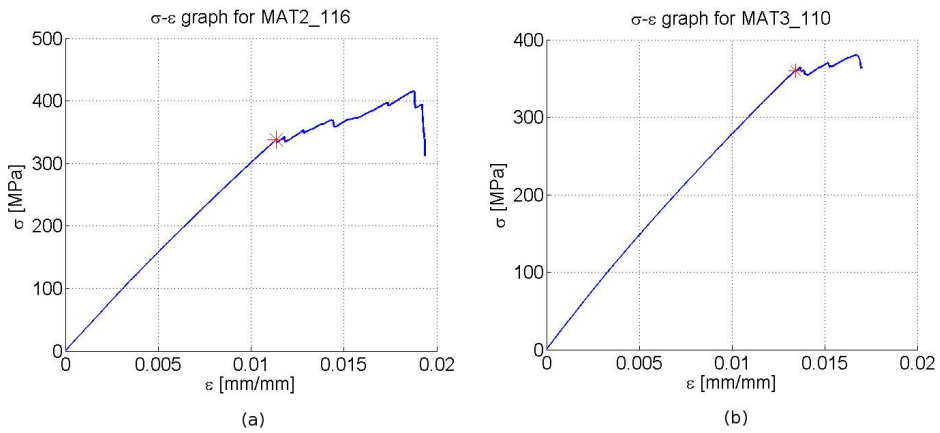


Figure 6: Stress-strain curves for a MAT2 and a MAT3 specimen

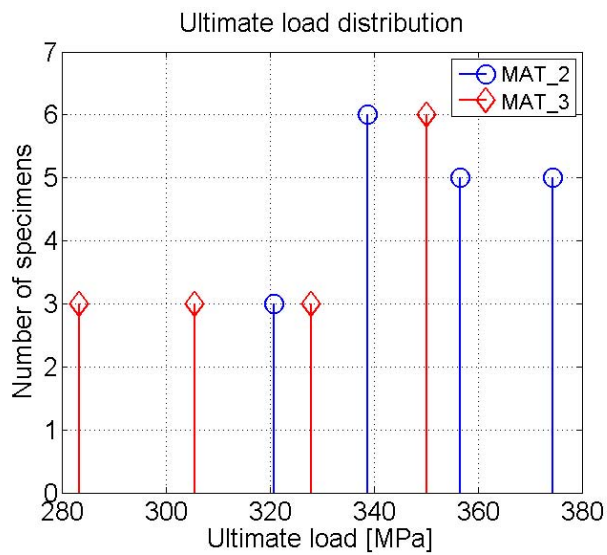


Figure 7: Ultimate load distribution

two materials can be seen, although MAT3 shows a lower mean value.

The elastic modulus showed indeed a difference between the two materials, which can be explained by considering the presence of the Volumat (which contributes partially to the longitudinal rigidity). Thus, a lower elastic modulus is measured in MAT3 specimens (Figure 8). In particular, MAT2 specimens showed a mean elastic modulus of 32500 MPa, where MAT3 specimens showed a mean value of 29600 MPa.

Broken specimens showed a uniform behavior, with an abrupt delamination failure mode which involves the MAT layer (Figure 9).

MAT3 specimens showed delaminations also extended to the inner MAT layer, which separated from the longitudinal fibers (Figure 10).

All specimens also presented some form of longitudinal cracking of the upper and lower MAT layers, which developed during the test and not as a result of the delamination (Figure 11).

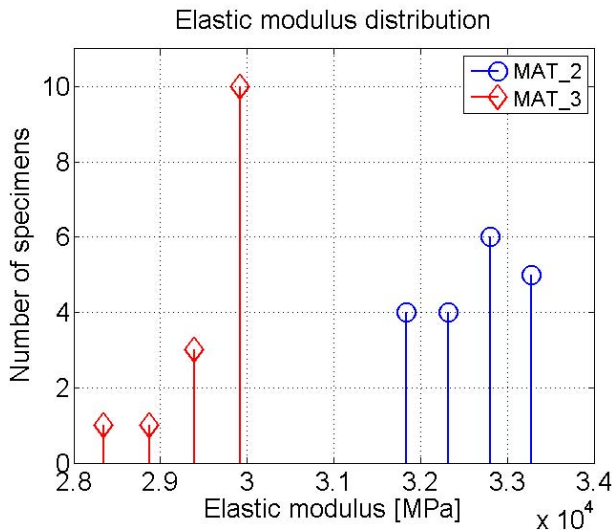


Figure 8: Elastic modulus distribution

These damage modes, as previously remarked, are found in the whole specimen set. In no case, inspection of the broken specimens showed massive fiber breakage inside the specimen.



Figure 9: Delamination of a specimen (MAT2)



Figure 10: Delamination of a specimen (MAT3)



Figure 11: Longitudinal MAT cracking

3.2 Acoustic Emission measurements

AE activity and behavior is comparable throughout the specimen set. As can be seen in Figure 12, the activity is low (i.e. a low number of events in time) in the first part, then the AE rate increases steadily; finally (after the first load drop) the activity slows down, in a S-shaped curve similar to the one found in [Carpenter and Kumosa (2000)].

AE cumulated energy parameter (Figure 13), on the other hand, shows a sudden increase prior to failure (the beginning of the inelastic regime). This is an indicator of catastrophic failure occurring in the specimen, with less events with an higher energy content.

The comparison between multiple AE events curves, normalized at the inelastic strain value ϵ_i , shows a different behavior between the two materials (Figure 14); in particular MAT3 seems to be more active than MAT2. This behavior is confirmed by the comparison of the first derivative (AE rate, Figure 15), which shows that the AE activity is not monotonically increasing but its derivative is also increasing, until it reaches a maximum before the breakage strain. This analysis shows also that MAT3 has its maximum AE rate (peak) at a strain which is lower than that of MAT2.

The most appealing feature of AE is the possibility to locate the damage location. The most promising feature for failure detection is cumulated AE energy; this can

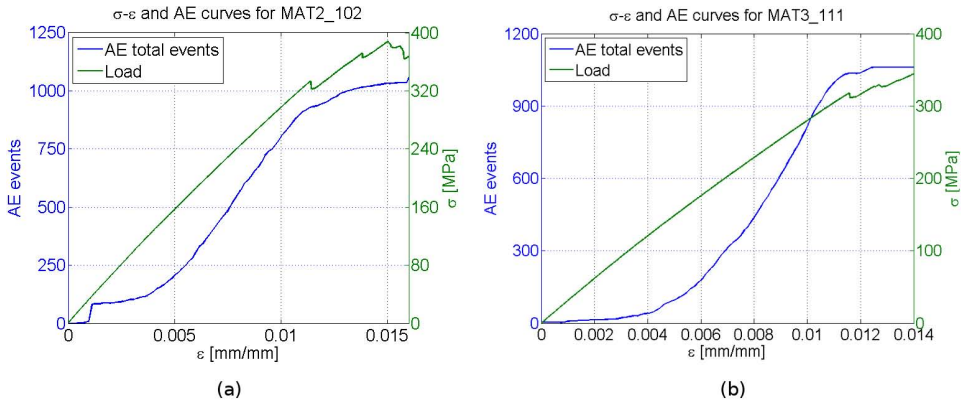


Figure 12: AE events and stress-strain curve for two specimens

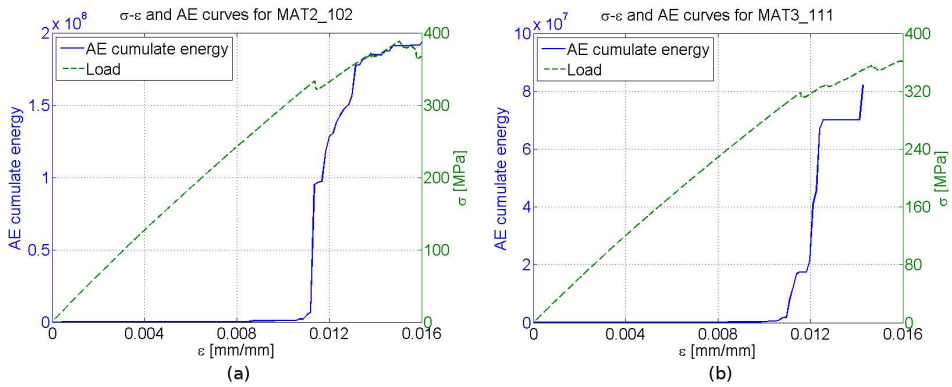


Figure 13: AE cumulated energy during two tests

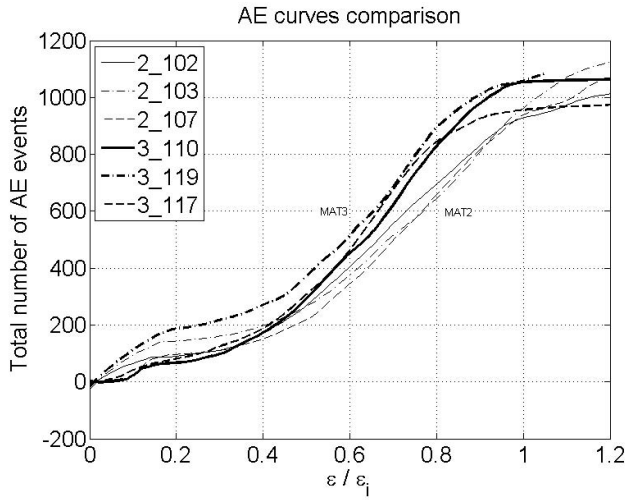


Figure 14: Comparison of AE curves of different specimens

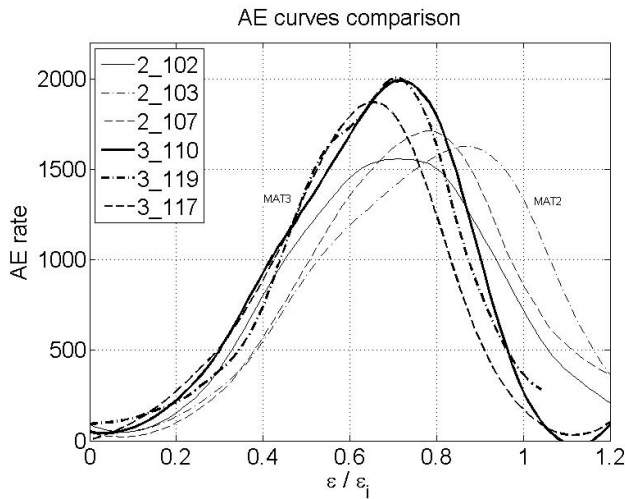


Figure 15: Comparison of the first derivative of AE activity of different specimens

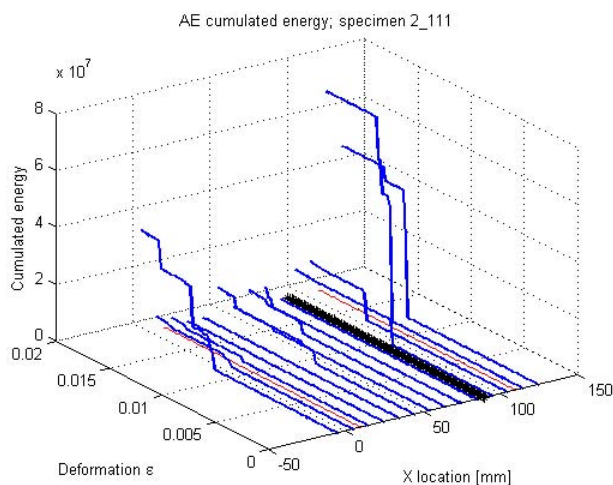


Figure 16: Progression in time of cumulated energy, divided by X location

be seen in Figure 16, that shows (in solid line) the AE cumulated energy for sections of 10mm width. In the case depicted, a MAT fracture was found at about 80mm (marked with a thick line in the xt plane), and confirmed by the energy released in that area.

4 Discussion and conclusions

The results of the tensile tests showed no appreciable differences between MAT3 and MAT2 specimens in terms of resistance. The different failure modes explained how the debonding / delamination of the MAT layers have a key role in static failure of the material; in particular, having these layers a different stiffness compared to the one of the longitudinal fiber layer, the different deformations may lead to this phenomenon.

The difference in elastic modulus is clearly explained by the lower content of unidirectional fibers in MAT3 specimens; this confirms that the rigidity of the MAT layers contributes negatively to the overall material stiffness in the main fiber direction.

AE results showed that the damage of this material is divided in 3 macro-phases: the first one, with lower AE activity (up to 70 MPa, which corresponds to the fatigue limit of the material [Vergani (2006)]) which presents a form of non-cumulative energy release, which may be linked to fiber-matrix friction phenomena; a second phase, with a steadily increasing AE ratio, where a more severe damage mode

occurs, that can be linked to the beginning of a decohesion mode, and a third phase, where the load carrying capacity of the material is no more evenly distributed, and causes the layers near to the load application surfaces to slip and delaminate.

This third phase is found to come earlier in MAT3 specimens, where the AE rate peak is also higher: this proves the ability of AE to distinguish the damage development of these materials. In fact, as underlined before, this type of layup consists of an additional Volumat layer in the middle of the specimen section, which is used to give to the material a better behavior in all the loading directions which are not parallel to the fiber axis. This type of AE signals may indicate that the decohesion phenomena are more severe because they involve a further discontinuity in the Volumat interface.

On the basis of the obtained results it can be concluded that Acoustic Emission can be considered a promising health monitoring technique for this kind of materials, with a good repeatability and a good estimation of failure location. This feature can be extended to the monitoring of a complex structure where sensors can be used to detect the position of a defect, and to monitor its severity.

The kind of AE setup used for this work doesn't allow location of events through the thickness of the specimen, which would be useful for a more precise assessment of damage modes. A solution to this is being investigated with the use of wavelet transform in uniform media [Hamstad (2009)], but the application to heterogeneous materials will require a deeper knowledge of wave propagation and reflection inside such media.

More advanced techniques can be used to separate the different damage modes (for example with neural networks) and to correctly define a monitoring method that can quantify the damage severity in a more reliable way.

References

ASTM International (2008): *ASTM D3039 - Standard test method for tensile properties of polymer matrix composite materials.*

ASTM International (2010): *ASTM E976 - Standard Guide for Determining the Reproducibility of Acoustic Emission Sensor Response.*

Carpenter, S. H. and Kumosa, M. (2000): An investigation of brittle fracture of composite insulator rods in an acid environment with either static or cyclic loading. *Journal of Materials Science*, vol. 35, no. 17, pp. 4465-4476.

Crivelli, D.; Guagliano, M.; Marangoni, D.; Monici, A. (2010): *Fatigue Damage Analysis of Pultruded Glass Fiber Reinforced Materials with Acoustic Emission Methods.* In Proceedings of EWGAE 2010, Vienna.

Finleyson, R. D. (2003): *Handbook of Nondestructive Evaluation*. McGraw-Hill Companies.

Grosse, C.; Ohtsu, M. (2008): *Acoustic Emission Testing*. Springer-Verlag Berlin Heidelberg.

Hamstad, M. A. (2009): Some observations on Rayleigh Waves and Acoustic Emission in Thick Steel Plates. *J. Acoustic Emission*, Vol. 27, pp. 114 – 136.

Huang M. et al. (1998): Using acoustic emission in fatigue and fracture materials research. *JOM*, vol. 50, pp. 1–12.

Jessen, S. M.; Plumtree, A. (1999): Fatigue damage accumulation in pultruded glass/polyester rods. *Composites*, vol 20, no. 6, pp. 559–567.

Keller, T. et al. (2005): Tensile fatigue performance of pultruded glass fiber reinforced polymer profiles. *Composite Structures*, vol 68, pp. 235–245.

Starr, T. (2000): *Pultrusion for Engineers*. Woodhead Publishing Ltd.

Takeda, S. et al (2007): Structural health monitoring of composite wing structure during durability test. *Composite structures*, vol. 79, pp. 133-139.

Vergani, L. (2006): *Damage mechanisms in pultruded unidirectional fiber reinforced composites under static and fatigue loads*. *Fracture and Damage of Composites*. WIT 2006, pp. 49–72.

